Propagation of a pressure step in a granular material: The role of wall friction

T. Boutreux, E. Raphaël, and P. G. de Gennes
Laboratoire de Physique de la Matière Condensée, CNRS URA No. 792, Collège de France, 11 place Marcelin Berthelot, 75231 Paris Cedex 05, France
(Received 3 October 1996)

More than one century ago Janssen [Z. Ver. Dtsch. Ing. **39**, 1045 (1895)] proposed an elegant model to describe the pressure variations in a vertical container filled with a granular material at rest. In the present paper we build up a dynamical version of this model. We analyze the propagation of a pressure front in a dry granular medium inside a cylinder, taking into account the solid friction that exists between the grains and the cylinder walls. Assuming that the granular material under pressure has a linear elastic behavior, we derive a linear partial differential equation for the pressure field. Using the Green function method, we determine analytically the behavior of the granular medium undergoing a pressure step. We find in particular that a pressure front propagates at speed c, the speed of sound in the granular material (within the linear elasticity framework, c is a constant). Due to friction at the cylinder walls, the front amplitude decays exponentially. We also show that a stopping front starts after a certain time lag and propagates behind the pressure front, at a speed larger than c. When reached by this second front, the grains stop and do not move any more. The final pressure profile that we predict when all grains have eventually stopped is similar, but not identical, to the pressure profile determined by the Janssen model. [S1063-651X(97)10905-9]

PACS number(s): 83.70.Fn, 46.10.+z, 46.30.Pa, 83.50.Tq

I. INTRODUCTION

Granular materials are ubiquitous in our daily lives and play an important role in many industrial and geophysical processes [1,2]. Over the last decades, many new ideas and techniques have been developed to understand the exceptional properties displayed by granular systems [3–7]. Even in the resting state, granular materials have unusual properties. Consider, for instance, a tall cylindrical container filled from the top with granular materials up to a height h. For h very small, the pressure p at the base of the container varies linearly with h, as would be the case for a normal fluid. However, the pressure p does not increase indefinitely as h increases. Instead, for a sufficiently tall column, p reaches a constant value that is independent of h. This easily observed phenomenon was explained by Janssen a long time ago [8]: because of static friction between the grains and the sides of the container, the container walls support the weight of the extra mass placed on the top of the column.

In this article we shall build up a dynamical version of the Janssen model. In order to do so, we shall consider a horizontal cylinder filled with a granular material. At a given time, say $t=0$, we shall impose a strong pressure at one end of the cylinder, and maintain it for $t>0$. We study how this pressure step propagates inside the cylinder. Our aim is to find out how the acoustic response to the pressure step is influenced by wall friction. In particular, we shall analyze how a steady Janssen-like pressure profile is reached for $t\to+\infty$. The phenomenon studied in this article is somewhat analogous to the ''water hammer'' pressure developed along a pipe by sudden closing of a tap [9]. The paper is organized as follows. In Sec. II we recall and discuss the Janssen model. Our dynamical model is then presented in Sec. III. In Sec. IV we solve the model analytically and show that the pressure step propagates inside the cylinder at the speed of sound of the bulk granular material. In Sec. V we show that a stopping front progressively invades the container, any slice of granular material coming eventually to rest. The final state of the system turns out to be similar, but not identical, to Janssen's state. The paper ends with some concluding remarks (Sec. VI).

II. THE JANSSEN MODEL

Let us review and discuss the Janssen model [8]. Consider a vertical cylinder of radius R filled with grains at rest. The granular medium is described by a continuum theory, and the aim of the model is to determine the pressure inside the material (induced by gravity) as a function of depth x (where the x axis is the cylinder axis, oriented downward). Note that the definition of ''pressure'' in a granular medium is tricky. A stress-induced birefringence technique [10–12] allows one to observe the distribution of forces within a compressed granular material. This technique shows a network of linear stress-transmitting paths, and regions with nearly no stress: the spatial fluctuations of the pressure are large. Moreover, many linear paths are parallel to some preferred directions: pressure is anisotropic. In order to take this anisotropy into account in the Janssen model, one defines two pressures, assumed to be constant over a horizontal plane: $p_g(x)$ acts on the horizontal surface between two grain slices (a grain slice is made of the grains located between two horizontal planes), and $p_c(x)$ acts between the vertical surfaces of slices and the cylinder inner sides. Because of the pressure anisotropy, $p_g(x)$ and $p_c(x)$ are *a priori* different. In order to simplify the problem, one assumes that these two pressures are proportional: $p_c(x)=Kp_g(x)$, where K is a constant. Let us now determine $p_g(x)$ by writing that a thin grain slice of thickness dx and at depth x is at rest. As shown in Fig. 1, the forces acting on this slice are (i) its weight $w=\pi R^2 dx\,\rho g$, where ρ is the grain density (assumed to be constant) and g the acceleration of gravity, (ii) the two pressure forces

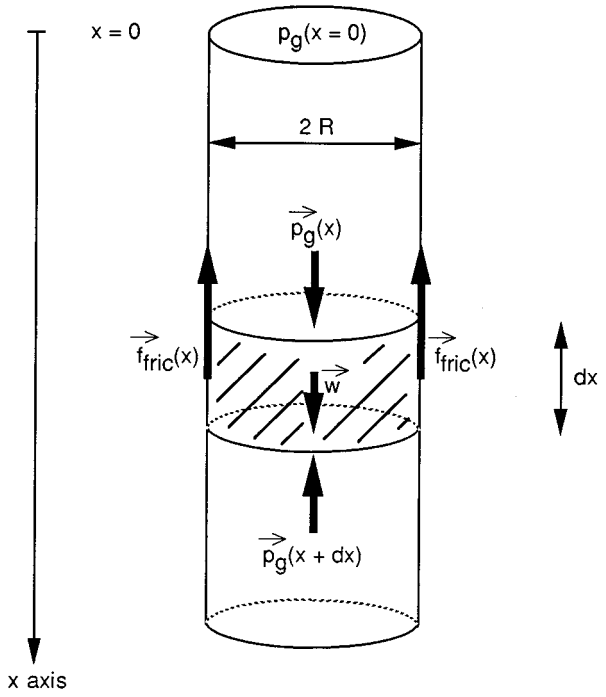

FIG. 1. In a vertical cylinder filled with grains at rest, the pressure $p_g(x)$ is calculated by writing the equilibrium of a grain slice of thickness dx at depth x. The forces acting on the slice are its weight $\vec{w}$, the vertical pressure forces $\vec{p}_g(x)$ and $\vec{p}_g(x+dx)$, and the solid static friction $\vec{f}_{\rm fric}(x)$ with the cylinder walls.

acting on top and bottom of the slice

$$\pi R^2[p_g(x)-p_g(x+dx)],$$

(iii) the solid static friction $f_{\rm fric}(x)$ of grains on the cylinder sides. According to the laws of static friction, $f_{\rm fric}(x)$ must satisfy the double inequality

$$-\mu f_p(x) \leqslant f_{\rm fric}(x) \leqslant +\mu f_p(x),$$

where μ is the friction coefficient between grains and the container sides, and $f_p(x)$ the pressure force of the slice on the sides: $f_p(x)=2\pi R dx p_c(x)$. In order to determine $f_{\rm fric}(x)$ we assume that the container has been filled from the top. When grains were poured, they moved downward and the (dynamic) friction force acted upward. We assume that when grains stopped, this force kept the same direction, and that grains at rest are about to slide down: friction is oriented upward, and its magnitude has the maximum value allowed by static friction; if grains were slightly pushed downward, friction would not be able to increase any more and grains would start to move. The friction force on the grain slice is thus given by

$$f_{\rm fric}(x) = -\mu f_p(x) = -\mu 2\pi R dx K p_g(x). \qquad (1)$$

The slice being at rest, the sum of the forces applied to it must be equal to zero,

$$\pi R^2 dx \rho g - \pi R^2 dx \frac{dp_g}{dx} - 2\pi R dx \mu K p_g = 0. \qquad (2)$$

Equation (2) can be rewritten as

$$\frac{dp_g(x)}{dx} + \frac{p_g(x)}{\lambda} = \rho g, \qquad (3)$$

where the characteristic length λ is given by

$$\lambda = \frac{R}{2\mu K}.$$

The length λ will play an important role throughout this article. In practice, for our problem, the order of magnitude of λ is $\lambda \sim 0.1$ m (as shown in Sec. III). Since the pressure in the material is inhomogeneous on the scale of a few grains but becomes homogeneous on the scale of, say, 50 or so grains, λ is a relevant length scale if the grain size is smaller than 1 mm. Equation (3) admits the solution

$$p_g(x) = \lambda\rho g + [p_g(x=0) - \lambda\rho g]\exp\left(-\frac{x}{\lambda}\right), \qquad (4)$$

where $p_g(x=0)$ is the pressure that we may impose at the top of the granular media. Equation (4) indicates that the pressure reaches exponentially the limit value $\lambda\rho g$, with a damping length given by λ. When x is larger than $\sim 3\lambda$, the pressure no longer varies because the cylinder sides support the extra weight of grains. This situation is very different from the case of a liquid, where the pressure increases linearly with depth. Note that the limit pressure $\lambda\rho g$ and the damping length λ are independent of both the pressure imposed at $x=0$ and the container height. In practice, μK is of order of 0.1 [13], so that $\lambda \approx 5R$. The pressure distribution of the Janssen model has been tested by different experiments [14,15]. In general, the pressure measured as a function of the depth has a shape similar to the Janssen pressure $p_g(x)$. Yet the value of the limit pressure at large depths can vary with an amplitude as large as 50%, and the pressure is influenced by the way the grains are poured in the cylinder and by the formation of stress arches supported by the container walls [16]. More details about these experiments can be found in Ref. [13].

We now generalize the Janssen model by relaxing the assumptions that grains were poured in the cylinder from the top and are about to slide down. The friction force $f_{\rm fric}(x)$ is no longer given by Eq. (1), but must only verify $-\mu f_p \leqslant f_{\rm fric} \leqslant +\mu f_p$, and Eq. (3) for the pressure $p_g(x)$ is now replaced by

$$-\frac{p_g(x)}{\lambda} \leqslant \frac{dp_g(x)}{dx} - \rho g \leqslant +\frac{p_g(x)}{\lambda}.$$

This generalization allows us to imagine new experiments where the pressure is very different from the Janssen pressure profile [17]. For instance, let us assume that we have an experimental setup which allows us to fill the container from the bottom by pushing up the grains; during this filling friction at the sides acts downward. If we suppose that when they stop, grains are about to slide up, we get $f_{\rm fric}(x) = +\mu f_p(x)$, and

$$p_g(x) = -\lambda\rho g + [p_g(x=0) + \lambda\rho g]\exp\left(+\frac{x}{\lambda}\right).$$

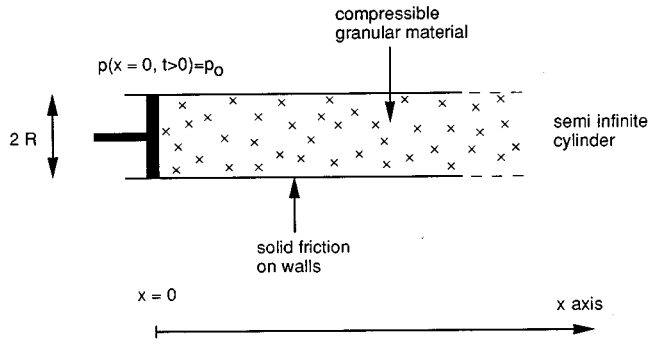

FIG. 2. The water hammer model for a granular material: at $t=0$, we apply a pressure step at the end of the horizontal cylinder.

Pressure increases exponentially with depth x, because the cylinder sides push grains downward. Another example is the experiment done in a cylinder with a friction coefficient μ_u in its upper part, and a larger friction coefficient μ_l in its lower part, so that $\lambda_l<\lambda_u$. We assume that the container was filled from the top, that grains at rest are about to slide down, and that $p_g(x=0)<\lambda_u\rho g$. When the depth x increases, the pressure first increases in the upper part of the cylinder from $p_g(x=0)$ to a first limit value $\lambda_u\rho g$, and then decreases exponentially in the lower part to a second limit value $\lambda_l\rho g$. These two examples show pressure distributions that are qualitatively very different from the Janssen one. This underlines both the richness and the complexity of the physics that mix continuum media and solid friction.

III. THE ''WATER HAMMER'' MODEL FOR A GRANULAR MATERIAL

A. The water hammer model

The Janssen model described in Sec. II was intrinsically static. We now want to build up a dynamical version of this model in order to show how a Janssen pressure profile can actually be reached. Making a model of a granular material being poured inside a vertical silo is complicated; we shall discuss such a filling in the conclusion of the present paper (Sec. VI). In this part of the article, let us consider the slightly different and simpler situation shown in Fig. 2. We first take a cylinder already filled with closely packed grains. We assume that the granular material is dry, and that there is no adhesion of grains to the container walls. Yet there is solid friction between the grains and these walls. Since we are not primarily interested in gravitational effects, we set the cylinder horizontally. Before the experiment begins, grains are at rest. At time $t=0$, we strongly increase the pressure of grains at one end of the cylinder, and thereafter keep constant the pressure at this end. In order to avoid complicated reflections on the other cylinder end, we assume that the container is semi-infinite. The pressure step propagation studied in this article is analogous to the water hammer phenomenon that happens in a pipe when a tap is suddenly closed [9].

As in the Janssen model, we assume that the granular material can be described by a continuum theory. Let us denote by $p(\vec{r},t)$ and $\vec{v}(\vec{r},t)$ the pressure and velocity of grains at position $\vec{r}$ and time t. We choose the Lagrangian description; for example, $p(\vec{r},t)$ is the pressure of the grain slice whose position was $\vec{r}$ at $t=0$. This pressure p acts on the vertical surfaces between two slices of the granular medium (it was denoted p_g in Sec. II). Let us call the cylinder axis the x axis; we take $x=0$ at the compressed end and $x>0$ in the semi-infinite container. We neglect the radial dependence of pressure and velocity and assume that the velocity is parallel to the x axis, so that pressure and velocity are simply given by two scalar functions of two variables: $p(x,t)$ and $v(x,t)$. By packing grains inside the cylinder before the experiment begins, we get a pressure $p(x\geqslant 0,t<0)$. Experimentally, this initial pressure may not be reproducible. Here, we assume that the pressure p_0 imposed at the cylinder end $x=0$ for $t\geqslant 0$ is much larger than the initial pressure, so that we can neglect it and get as first initial condition in our model $p(x>0,t=0)=0$. Because grains are at rest before the experiment begins, a second initial condition is $v(x>0,t=0)=0$.

In order to describe the dynamics of grains, we first write the momentum conservation law for a grain slice located between x and $x+dx$. Two forces act on the slice: a solid friction force and pressure forces (gravity being neglected). The pressure forces act on the two vertical sides of the slice, and their sum is equal to

$$\pi R^2[p(x,t)-p(x+dx,t)],$$

where R is the cylinder radius. When the slice is moving, the dynamic friction force of grains on the cylinder sides has a magnitude equal to μf_p, where f_p is the pressure force exerted by the grain slice on the container sides and μ is a friction coefficient assumed to be independent of the speed v. Moreover, we assume that this coefficient is equal to the static friction coefficient of Sec. II. Introducing a new dynamic friction coefficient is easy, but would make our equations more complicated and would not qualitatively change our predictions. The pressure force f_p is equal to $2\pi RdxKp$, where the constant K reflects the pressure anisotropy of the granular medium (see Sec. II). Since grains are pushed towards the positive x direction, v is positive and the sign of the friction force is negative. The dynamic friction force acting on the slice is thus equal to

$$-\mu 2\pi RdxKp.$$

If the slice is at rest, the friction force becomes static, and can take any value between $-\mu 2\pi RdxKp$ and $+\mu 2\pi RdxKp$. The consequences of this nonlinear behavior of the friction force will be studied in detail below.

According to the momentum conservation law, in the elastic approximation (see below) and when the slice is moving, we have

$$\pi R^2 dx\rho\frac{\partial v}{\partial t}=-\pi R^2 dx\frac{\partial p}{\partial x}-2\pi Rdx\mu Kp,$$

where ρ is the grain density, assumed to be constant. By dividing the above equation by $\pi R^2 dx$, we get

$$\rho\frac{\partial v}{\partial t}=-\frac{\partial p}{\partial x}-\frac{p}{\lambda}, \tag{5}$$

where λ is given by $\lambda = R/(2\mu K)$ as in Sec. II. Note that Eq. (5) is also valid for a grain slice before it starts to move: in this case $p=0$ and there is no friction between the slice and the wall.

Another differential equation comes from the assumption that the granular medium under pressure has an elastic response. A grain slice of initial volume V will have a smaller volume $V+\Delta V$ for $p>0$ with ΔV given by

$$\frac{p}{\tilde{E}} = \left(-\frac{\Delta V}{V} \right)^m , \tag{6}$$

where the elastic modulus $\tilde{E}$ and the exponent m are assumed to be constant. This elastic model is valid if two conditions are fulfilled: First, the grains must be sufficiently packed before we impose the pressure step so that we can neglect the special behaviors displayed by granular materials when the grains are barely touching [3]. Secondly, at $t \geqslant 0$, we must keep $|\Delta V| \ll V$, i.e., $p \ll \tilde{E}$; this will be the case in the solution obtained in Sec. IV. The exact value of the exponent m appearing in Eq. (6) has been the subject of many studies. By assuming that the grain surface is smooth and that the contacts between grains are Hertzian, one obtains $m=3/2$ [18]. Yet experiments [19] have shown that a better exponent to fit the data is $m=2$. Various theoretical explanations for this value have been proposed recently [18,20]. Since our aim in the present paper is to study the influence of wall friction on the acoustic response of the material, we will make the simplest choice, $m=1$. By differentiating Eq. (6) (written for a thin grain slice of thickness dx) with respect to time, we get another differential equation describing the grain dynamics,

$$\frac{\partial v}{\partial x} = -\frac{1}{\tilde{E}} \frac{\partial p}{\partial t} . \tag{7}$$

To summarize, our model leads to two coupled differential equations (7) and (5), along with the initial conditions $p(x>0,t=0)=0$ and $v(x>0,t=0)=0$, and the boundary condition $p(x=0,t \geqslant 0)=p_0$. Note that in the absence of wall friction ($1/\lambda = 0$), Eq. (5) reduces to $\rho \partial v/\partial t = -\partial p/\partial x$. By combining this expression and Eq. (7), we obtain

$$\rho \frac{\partial^2 p}{\partial t^2} = \tilde{E} \frac{\partial^2 p}{\partial x^2} .$$

The solutions of this equation are simple acoustic waves propagating at the speed of sound $c=(\tilde{E}/\rho)^{1/2}$. The fact that the speed of sound is a constant is a direct consequence of the linear assumption ($m=1$) in Eq. (6). In the granular medium undergoing the pressure step p_0, the pressure front propagates at speed c with a constant amplitude; grains ahead of the front are at rest; the pressure in the grains behind the front is constant and equal to p_0, and these grains move at a uniform and constant speed. As we shall see, the introduction of friction significantly complicates the resolution of the problem, and leads to new phenomena.

B. Orders of magnitude of the physical phenomena

Equations (7) and (5), along with their initial and boundary conditions, will be analytically solved in Sec. IV. Let us first show that it is possible to determine *a priori* most of the orders of magnitude of the physical phenomena. Equations (7) and (5), as well as the initial conditions and the boundary condition, depend on the four physical parameters ρ, c, λ, and p_0. We can thus define four dimensionless quantities

$$x^* = \frac{x}{\lambda}, \quad t^* = \frac{c}{\lambda} t, \quad p^* = \frac{p}{p_0}, \quad \text{and} \quad v^* = \frac{\rho c}{p_0} v .$$

If we rewrite Eqs. (7) and (5) in terms of the above dimensionless quantities, we get

$$\frac{\partial v^*}{\partial t^*} = -\frac{\partial p^*}{\partial x^*} - p^*$$

and

$$\frac{\partial v^*}{\partial x^*} = -\frac{\partial p^*}{\partial t^*} ,$$

along with the initial conditions $p^*(x^*>0,t^*=0)=0$ and $v^*(x^*>0,t^*=0)=0$, and the boundary condition $p^*(x^*=0,t^* \geqslant 0)=1$. These dimensionless equations and conditions define a new problem that does not depend on any physical parameter any more. Any quantity of the solution of this dimensionless problem must be of the order of 1, because the only constraint is the boundary condition $p^*(x^*=0,t^* \geqslant 0)=1$. Moreover, the solution of the model with dimensions can be found easily from the solution of the dimensionless problem. For instance, the pressure $p(x,t)$ is given by $p(x,t)=p_0 p^*(x/\lambda, tc/\lambda)$. Hence the orders of magnitude of the physical quantities in the model with dimensions are the following ones. The order of magnitude of the pressure is $p \sim p_0$, the order of magnitude of the grain speed is $v \sim p_0/\rho c$, the order of magnitude of the distance on which p and v vary is $x \sim \lambda$, the order of magnitude of the time during which p and v vary is $t \sim \lambda/c$, and finally the order of magnitude of the displacement of a grain slice is $\Delta l \sim v t \sim \lambda p_0/\rho c^2$.

For usual granular materials, the orders of magnitude of ρ and c are given by $\rho \sim 2 \times 10^3$ kg/m^3 and $c \sim 5 \times 10^2$ m/s [19,21]. Moreover, λ is of the order of $5R$ since $\lambda = R/(2\mu K)$ and the order of magnitude of μK is 0.1 (cf. Sec. II). As shown later, one has to choose R in the range $1-10$ cm for practical reasons. So the order of magnitude of λ is also determined: $\lambda \sim 0.1$ m. The order of magnitude of the time of variation is then given by $t \sim 0.2$ ms. The amplitude p_0 of the pressure step can be varied within a wide range, however. One has to keep $p_0 \ll \tilde{E} = \rho c^2 \sim 10^8$ Pa, and p_0 must be larger than a minimum value: the magnitude of the friction force was determined because grains were moving. This is the case provided that the minimum grain displacement $\Delta l_{\min}$ is larger than the typical size of microscopic contacts between solids or grains, i.e., a few micrometers [22]. Hence the condition

$$\Delta l_{\min} \sim \frac{\lambda p_{\min}}{\rho c^2} > 5 \ \mu\text{m}.$$

The analytical solution of our model (Sec. IV) will show that $p_{\min} \sim p_0/50$. So we must have $p_0 > 10$ atm. A good choice is $p_0 \sim 10$–20 atm: it fulfills the above two inequalities, and should be easily feasible in practice. The order of magnitude of the grain speed is then $v \sim 1$ m/s, and the order of magnitude of the displacement of a slice under the pressure p_0 is $\Delta l \sim 0.3$ mm. Grain motions along the x axis are small and probably difficult to measure. Measurements should focus on the propagation of the pressure step, created, for instance, by the quick opening of a pressurized gas bottle. Fast captors should measure pressure on the outside cylinder surface, along a distance of 0.5–1 m [23].

IV. ANALYTICAL RESOLUTION—PROPAGATION OF A PRESSURE FRONT

A. Analytical resolution

In this subsection we shall analytically calculate the pressure p and the speed v of grains in a semi-infinite cylinder on which we impose a pressure step at $x=0$ and $t=0$; we shall solve the two partial differential equations (7) and (5). We shall first determine the function $p(x,t)$, and then $v(x,t)$ will easily be calculated by using Eq. (7). Combining Eqs. (7) and (5) leads to

$$\frac{1}{c^2}\frac{\partial^2 p}{\partial t^2} - \frac{\partial^2 p}{\partial x^2} - \frac{1}{\lambda}\frac{\partial p}{\partial x} = 0, \tag{8}$$

where $c = (\tilde{E}/\rho)^{1/2}$. Moreover, $p(x,t)$ must satisfy the boundary condition

$$p(x=0, t \geqslant 0) = p_0, \tag{9}$$

and the following two initial conditions:

$$p(x>0, t=0) = 0, \tag{10}$$

$$\frac{\partial p}{\partial t}(x>0, t=0) = 0. \tag{11}$$

The initial condition (11) results from Eq. (7) and the condition $v(x>0, t=0)=0$. The resolution of the differential equation (8) with the three conditions (9)–(11) will be called problem (P).

Note that our central equation (8) is somewhat different from the well-known telegraphist's equation [24], in which the term $\partial p/\partial x$ is replaced by $\partial p/\partial t$.

In order to solve problem (P), we will proceed in three successive steps. By using the Green function method, we will calculate the behavior of grains under an applied external excitation. In a second step, this behavior will allow us to solve the Cauchy problem for the pressure inside a granular medium in an infinite cylinder. The last step will be to solve problem (P) by using the solution of the Cauchy problem. We will not explain all the mathematical details of our calculations. We use standard methods of mathematical physics; rigorous explanations can be found in Refs. [24,25]. We will mostly try to emphasize the physical meaning of the methods we use; detailed mathematical calculations are presented in Appendixes A–C.

1. Response to an external excitation

As a first step towards the resolution of problem (P), let us study the response to an external excitation of grains in an infinite cylinder (i.e., a cylinder extended in both positive and negative x directions). The external excitation is as follows: let us assume that on a grain slice of thickness dx and at position x, we can exert an external force $f(x,t)dx$ at time t. We assume that for $t<0$ the force $f(x,t)$ is equal to zero; therefore the grains are at rest (for $t<0$) and $p_A(x, t<0) = 0$. The pressure in the material is denoted by p_A for reasons that will soon become clear. Because of the external force for $t \geqslant 0$, grains start to move and pressure changes. The momentum conservation law, which led to Eq. (5), now yields

$$\rho \frac{\partial v}{\partial t} = -\frac{\partial p_A}{\partial x} - \frac{p_A}{\lambda} + \frac{f}{\pi R^2}.$$

Equation (8) then becomes

$$\frac{1}{c^2}\frac{\partial^2 p_A}{\partial t^2} - \frac{\partial^2 p_A}{\partial x^2} - \frac{1}{\lambda}\frac{\partial p_A}{\partial x} = A, \tag{12}$$

where $A(x,t) = -(1/\pi R^2)\partial f/\partial x$ is called the external excitation. We want to calculate $p_A(x,t)$ as a function of $A(x,t)$. Since Eq. (12) is a linear equation with constant coefficients, its solution p_A is given by [25]

$$p_A(x,t) = A(x,t) * G(x,t),$$

where the symbol $*$ denotes a convolution product; the function $G(x,t)$ is called the Green function of Eq. (8). If the excitation were proportional to an impulsive force at $x=0$ and $t=0$, i.e., $A(x,t) = a\,\delta(x)\,\delta(t)$ where δ is the Dirac delta function and a an arbitrary constant used so that A has the correct dimension, then the pressure would be

$$p_A(x,t) = [a\,\delta(x)\,\delta(t)] * G(x,t) = a\,G(x,t).$$

The Green function $G(x,t)$ is thus proportional to the pressure in the grains when we apply an impulsive force to the material. The calculation of this pressure can be done by a Fourier transform with respect to x. This calculation is presented in Appendix A. We find that the Green function of Eq. (8) is given by

$$G(x,t) = \frac{c}{2}\,\theta(ct - |x|)\exp\left(-\frac{x}{2\lambda}\right) J_0\left(\frac{\sqrt{c^2t^2 - x^2}}{2\lambda}\right),$$

where J_0 is a Bessel function of the first kind [26], and θ the Heaviside unit step function. Note that since the Bessel function J_0 is oscillatory, the Green function $G(x,t)$ takes both positive and negative values. However, as we shall see later (in Sec. V), the physical solution $p(x,t)$ of problem (P) is always positive (as it should be in a noncohesive granular material).

2. The Cauchy problem for the pressure

In a second step towards the resolution of problem (P), let us solve the Cauchy problem for the pressure p_C in an infinite cylinder filled with grains, by using the Green function G. We consider that at time $t=0$, we know $p_C(x,t=0)$ and its first derivative with respect to time, $(\partial p_C/\partial t)(x,t=0)$. We want to calculate $p_C(x,t)$ for $t\geqslant 0$, assuming that for $t\geqslant 0$ there is no external excitation; $p_C(x,t)$ is then a solution of Eq. (8). This calculation can be done by using the grain response to an external excitation, determined in the preceding paragraph. We are going to show that we can find an excitation $A(x,t)$ which is equal to zero when $t\neq 0$ but is singular for $t=0$, so that the solution $p_A(x,t)$ of the external excitation problem will verify the following conditions: (i) for $t<0$, $A=0$, the grains are at rest and $p_A(x,t)=0$; (ii) at $t=0$, the excitation A changes instantaneously the state of the grains from rest to a state characterized by the initial conditions of the Cauchy problem, i.e., $p_A(x,t=0^+)=p_C(x,t=0^+)$ and $(\partial p_A/\partial x)(x,t=0^+)=(\partial p_C/\partial x)(x,t=0^+)$; and (iii) for $t>0$, $p_A(x,t)=p_C(x,t)$ (indeed, since $A=0$, both pressures verify the same differential equation).

If we can find such an excitation A, the solution of the Cauchy problem for $t>0$ will be equal to the solution of the external excitation problem, which can be calculated by a convolution product.

Let us determine the excitation $A(x,t)$. We must have

$$p_A(x,t)=\theta(t)p_C(x,t),$$

where p_A is a solution of Eq. (12) which includes A, and p_C is a solution of Eq. (8) which does not include any excitation. The last equation yields

$$\left(\frac{1}{c^2}\frac{\partial^2}{\partial t^2}-\frac{\partial^2}{\partial x^2}-\frac{1}{\lambda}\frac{\partial}{\partial x}\right)p_A = \theta(t)\left(\frac{1}{c^2}\frac{\partial^2}{\partial t^2}-\frac{\partial^2}{\partial x^2}-\frac{1}{\lambda}\frac{\partial}{\partial x}\right)p_C+\frac{1}{c^2}\delta(t)\frac{\partial p_C}{\partial t}(x,t=0) + \frac{1}{c^2}\delta'(t)p_C(x,t=0).$$

Since p_C is a solution of Eq. (8), we simply get

$$\left(\frac{1}{c^2}\frac{\partial^2}{\partial t^2}-\frac{\partial^2}{\partial x^2}-\frac{1}{\lambda}\frac{\partial}{\partial x}\right)p_A = \frac{1}{c^2}\left[\delta(t)\frac{\partial p_C}{\partial t}(x,t=0)+\delta'(t)p_C(x,t=0)\right].$$

Hence the singular excitation we want to determine is given by

$$A(x,t)=\frac{1}{c^2}\left[\delta(t)\frac{\partial p_C}{\partial t}(x,t=0)+\delta'(t)p_C(x,t=0)\right].$$

The solution of the Cauchy problem for $t\geqslant 0$ is equal to the convolution product of A by the Green function $G(x,t)$ calculated in the preceding paragraph,

$$p_C(x,t\geqslant 0)=A(x,t)*G(x,t)=\frac{1}{c^2}\left[\delta(t)\frac{\partial p_C}{\partial t}(x,t=0)+\delta'(t)p_C(x,t=0)\right]*\left[\frac{c}{2}\,\theta(ct-|x|)\exp\left(-\frac{x}{2\lambda}\right)J_0\left(\frac{\sqrt{c^2t^2-x^2}}{2\lambda}\right)\right].$$

The calculation of this convolution product is presented in Appendix B. We find that the solution of the Cauchy problem is given by

$$\begin{aligned}p_C(x,t\geqslant 0)=&\frac{1}{2c}\int_{x-ct}^{x+ct}dx'\,\frac{\partial p_C}{\partial t}(x',0)\exp\left(\frac{x'-x}{2\lambda}\right)J_0\left(\frac{\sqrt{c^2t^2-(x'-x)^2}}{2\lambda}\right)\\&-\frac{ct}{4\lambda}\int_{x-ct}^{x+ct}dx'\,p_C(x',0)\exp\left(\frac{x'-x}{2\lambda}\right)\frac{J_1\left((1/2\lambda)\sqrt{c^2t^2-(x'-x)^2}\right)}{\sqrt{c^2t^2-(x'-x)^2}}\\&+\frac{1}{2}\left[p_C(x+ct,0)\exp\left(\frac{ct}{2\lambda}\right)+p_C(x-ct,0)\exp\left(-\frac{ct}{2\lambda}\right)\right],\end{aligned}\tag{13}$$

where J_1 is a Bessel function of the first kind [26].

3. The analytical solution of problem (P)

We are now able to determine the pressure $p(x,t)$ that is the solution of problem (P), by using the solution of the Cauchy problem calculated in the preceding paragraph. Any particular choice for $p_C(x,t=0)$ and $(\partial p_C/\partial t)(x,t=0)$ (where $x\leqslant 0$ and $x\geqslant 0$) generates a solution $p_C(x,t)$ of Eq. (8), the differential equation of problem (P). For problem (P), let us look for a solution $p(x,t)$ of the following kind: $p(x,t)=k+p_C(x,t)$, where k is a constant. p and p_C will be mathematically defined for x both positive and negative, but only the part $x\geqslant 0$ of the function p will have a physical meaning in our model. We must determine the two functions $p_C(x,t=0)$, $(\partial p_C/\partial t)(x,t=0)$, and the constant k in order that $p(x,t)$ fulfills the boundary condition and the initial conditions of problem (P). Let us first consider the boundary condition: at $x=0$, the pressure $p_C(x,t)$ of any solution of the Cauchy problem can be written

$$p_C(x=0,t)=\frac{1}{2}\left[p_C(ct,0)\exp\left(\frac{ct}{2\lambda}\right)+p_C(-ct,0)\exp\left(-\frac{ct}{2\lambda}\right)\right]+\frac{1}{2c}\int_0^{ct}dx'\left[\frac{\partial p_C}{\partial t}(x',0)\exp\left(\frac{x'}{2\lambda}\right)+\frac{\partial p_C}{\partial t}(-x',0)\right.$$
$$\left.\times\exp\left(-\frac{x'}{2\lambda}\right)\right]J_0\left(\frac{\sqrt{c^2t^2-x'^2}}{2\lambda}\right)-\frac{ct}{4\lambda}\int_0^{ct}dx'\left[p_C(x',0)\exp\left(\frac{x'}{2\lambda}\right)+p_C(-x',0)\exp\left(-\frac{x'}{2\lambda}\right)\right]\frac{J_1((1/2\lambda)\sqrt{c^2t^2-x'^2})}{\sqrt{c^2t^2-x'^2}}.$$

If we impose that

$$p_C(x,t=0)\exp\left(\frac{x}{2\lambda}\right)+p_C(-x,t=0)\exp\left(-\frac{x}{2\lambda}\right)=0, \tag{14}$$

and that

$$\frac{\partial p_C}{\partial t}(x,t=0)\exp\left(\frac{x}{2\lambda}\right)+\frac{\partial p_C}{\partial t}(-x,t=0)\exp\left(-\frac{x}{2\lambda}\right)=0, \tag{15}$$

then we get $p_C(x=0,t)=0$. In addition, we take $k=p_0$, and the boundary condition $p(x=0,t\geqslant 0)=p_0$ is fulfilled. We still have to choose the functions $p_C(x,t=0)$ and $(\partial p_C/\partial t)(x,t=0)$ for $x>0$; the conditions (14) and (15) will then determine these functions for $x<0$.

Now let us consider the two initial conditions. The first condition $p(x>0,t=0)=0$ is fulfilled if we choose $p_C(x>0,t=0)=p(x>0,t=0)-p_0=-p_0$; then Eq. (14) imposes that $p_C(x<0,t=0)=+p_0\exp(-x/\lambda)$. The second initial condition $(\partial p/\partial t)(x>0,t=0)=0$ is fulfilled if we choose $(\partial p_C/\partial t)(x>0,t=0)=(\partial p/\partial t)(x>0,t=0)=0$, and then Eq. (15) imposes that $(\partial p_C/\partial t)(x<0,t=0)=0$. The solution $p(x,t)$ of problem (P) is then given by

$$p(x,t\geqslant 0)=p_0+\frac{1}{2}\left[p_C(x+ct,0)\exp\left(\frac{ct}{2\lambda}\right)+p_C(x-ct,0)\right.$$
$$\left.\times\exp\left(-\frac{ct}{2\lambda}\right)\right]-\frac{ct}{4\lambda}\int_{x-ct}^{x+ct}dx'\,p_C(x',0)$$
$$\times\exp\left(\frac{x'-x}{2\lambda}\right)\frac{J_1((1/2\lambda)\sqrt{c^2t^2-(x'-x)^2})}{\sqrt{c^2t^2-(x'-x)^2}}, \tag{16}$$

where

$$p_C(x,0)=\begin{cases} p_0\exp\left(-\dfrac{x}{\lambda}\right) & \text{if } x<0 \\ -p_0 & \text{if } x>0. \end{cases}$$

We have verified the validity of the above calculations by comparing the analytical solution (16) with a direct numerical integration of problem (P). This numerical integration was done—starting from Eqs. (7) and (5)—by using a finite difference method, with a Lax-Wendroff algorithm [27,28]. Note that this numerical scheme does not rely on the Green function method used to obtain Eq. (16). The agreement found between the numerical integration and the analytical solution is very good (the difference being less than 1%).

B. Propagation of a pressure front

The solution (13) of the Cauchy problem shows that the pressure at position x and time t is determined by the pressure and pressure time derivative at all points x' located between $x-ct$ and $x+ct$ at time $t'=0$. The pressure at a point x and time t cannot be influenced by the pressure and its derivative at another point (x',t') if this second point is ''outside the light cone'' of the first one, i.e., if $|x-x'|>c|t-t'|$. Hence, for a pressure step imposed at $x=0$ and $t=0$ in a semi-infinite cylinder, we have

$$p\left(x,t<\frac{x}{c}\right)=0.$$

This result can be checked directly by using expression (16). Moreover, for $t\geqslant x/c$ it is possible to simplify expression (16) further. Calculations are presented in Appendix C, and lead to

$$p\left(x,t\geqslant\frac{x}{c}\right)=p_0\exp\left(-\frac{x}{2\lambda}\right)\left[\cosh\left(\frac{ct-x}{2\lambda}\right)-\frac{ct}{2\lambda}\right.$$
$$\left.\times\int_{x/ct}^1 dz\cosh\left(\frac{zct-x}{2\lambda}\right)\frac{J_1((ct/2\lambda)\sqrt{1-z^2})}{\sqrt{1-z^2}}\right]. \tag{17}$$

This expression shows that $p(x,t=x/c)=p_0\exp(-x/2\lambda)$: a pressure front is generated by the step we impose at $x=0$, and propagates in the positive x direction at the speed of sound c. When the front arrives at a given point x, the pressure jumps from 0 to $p_0\exp(-x/2\lambda)$. Hence, despite the grain friction on the cylinder sides, we predict that a pressure discontinuity propagates at speed c, as in the frictionless case $(1/\lambda=0)$; the effect of friction on the front is to exponentially damp the pressure discontinuity. Note that the dynamic damping length 2λ at the front is larger than the static damping length λ of the Janssen model (cf. Sec. II). Since pressure is not continuous at $x=ct$, we must distinguish between the point of abscissa $x=ct^-$ just behind the front where $p(x=ct^-,t)=p_0\exp(-x/2\lambda)$, and the point of abscissa $x=ct^+$ just ahead of the front where $p(x=ct^+,t)=0$.

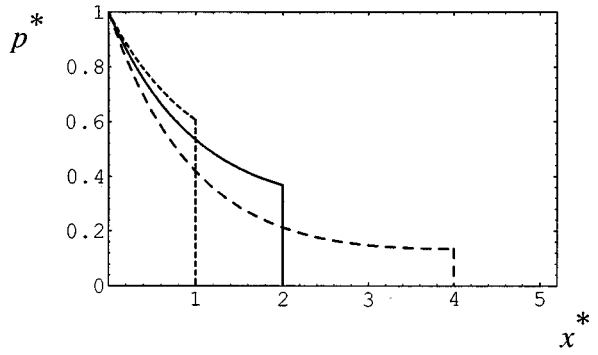

FIG. 3. Dimensionless pressure $p^*=p(x,t)/p_0$, solution of Eqs. (5) and (7), as a function of the dimensionless abscissa $x^*=x/\lambda$, at three different times: $t=\lambda/c$ (short dashed curve), $t=2\lambda/c$ (solid curve), and $t=4\lambda/c$ (long dashed curve). The discontinuities at the right ends of the curves correspond to the pressure front.

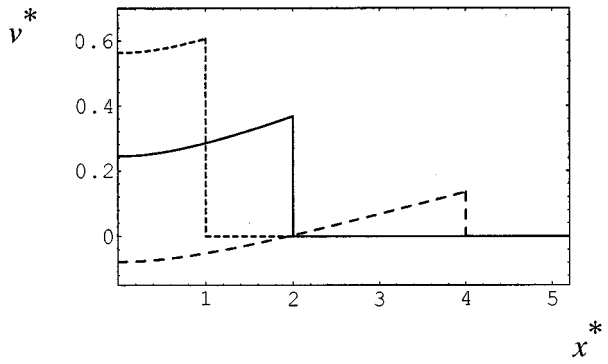

FIG. 4. Dimensionless velocity $v^*=v(x,t)\rho c/p_0$, solution of Eqs. (5) and (7), as a function of the dimensionless abscissa $x^*=x/\lambda$, for three values of the time t: $t=\lambda/c$ (short dashed curve), $t=2\lambda/c$ (solid curve), and $t=4\lambda/c$ (long dashed curve). As in Fig. 3, the sudden drops correspond to the speed discontinuity due to the pressure front. At a given abscissa and after the pressure front has passed, the velocity decreases and becomes negative as time increases.

Let us show that the pressure front corresponds also to a discontinuity in the grain velocity. The velocity can be calculated directly from Eq. (7),

$$\begin{aligned} v(x,t) &= -\frac{1}{\rho c^2}\int_{\infty}^{x}\frac{\partial p}{\partial t}(x',t)dx' \\ &= \frac{1}{\rho c^2}\int_{x}^{ct^+}\frac{\partial p}{\partial t}(x',t)dx' \\ &= \frac{1}{\rho c}p(x'=ct^-,t)+\frac{1}{\rho c^2}\int_{x}^{ct^-}\frac{\partial p}{\partial t}(x',t)dx' \\ &= \frac{p_0}{\rho c}\exp\left(-\frac{ct}{2\lambda}\right)+\frac{1}{\rho c^2}\int_{x}^{ct^-}\frac{\partial p}{\partial t}(x',t)dx'. \end{aligned} \quad (18)$$

When the front arrives, the velocity jumps from $v(x=ct^+,t)=0$ to $v(x=ct^-,t)=(p_0/\rho c)\exp(-x/2\lambda)$. Moreover, numerical integrations of expressions (17) and (18) show that at a given point of abscissa x, pressure and velocity decrease with a characteristic time of a few λ/c after the jumps occurring at $t=x/c$. This behavior is shown in Figs. 3 and 4, where pressure and speed are plotted against the abscissa x for $t=\lambda/c$, $2\lambda/c$, and $4\lambda/c$.

V. PROPAGATION OF A STOPPING FRONT

Figure 4 shows that according to the analytical solution (17), the velocity at $x=0$ becomes negative for t larger than $\sim 3\lambda/c$. A precise numerical calculation shows that this effect starts at $t_s=3.25\lambda/c$. For $t>t_s$, the velocity is negative between $x=0$ and a point where $v=0$. We will call the abscissa of this point $x_s(t)$; Fig. 4 shows that, for instance, $x_s(t=4\lambda/c)\approx 1.9\lambda$. The grains at $x>x_s(t)$ still have a positive speed. The point x_s has a positive velocity, i.e., the region where $v<0$ expands. However, this description cannot be valid, because in our equations we had assumed that all grains had a positive velocity: in Eq. (5), the term $-p/\lambda$ represents the force acting on grains due to their friction on the cylinder sides (cf. Sec. III). This term is negative because friction and velocity always have opposite directions, and we assumed that $v>0$. The analytical solution that we found contradicts this assumption for $t>t_s$. Our model and its analytical solution are valid everywhere in the granular material for $t<t_s$, and only in the part of the granular material in which $v>0$ for $t>t_s$. Elsewhere, they must be modified.

In order to understand what happens in the part of the granular material in which $v<0$, we must analyze more precisely the role of friction forces. When a grain slice stops ($v=0$) at $x=x_s(t)$, the friction applied on the slice by the cylinder is not dynamic any more, but becomes static. The solid friction laws do not determine the magnitude of this static friction force, but only require that it is inferior to the magnitude the force would have if the slice were moving,

$$|f_{\text{stat}}| \leqslant \frac{p}{\lambda}, \quad (19)$$

where f_{stat} is equal to the static friction force divided by the volume of the grain slice. f_{stat} can be calculated with the momentum conservation law. If condition (19) is fulfilled, the slice that stopped stays at rest; if Eq. (19) is not fulfilled, the static friction force needed to maintain the slice at rest is too large, and the slice motion must start again. To see if friction is sufficient to maintain the grain slices at rest, we calculate the magnitude of the static friction at $x<x_s$, assuming that grains definitively stop when the point $x_s(t)$ arrives [hypothesis (H)], and then we check if this magnitude verifies Eq. (19). If a grain slice definitively stops at a time t_0, its pressure will not change any more at $t>t_0$ and will keep the value it had at t_0. This allows us to calculate the pressure $p_s(x)$ of the grains that have stopped, by using the analytical solution (17). The function $p_s(x)$ is represented in Fig. 5 by a solid curve. The magnitude of static friction is then determined by the momentum conservation law [cf. Eq. (5)]

$$0 = -\frac{dp_s}{dx} + f_{\text{stat}}. \quad (20)$$

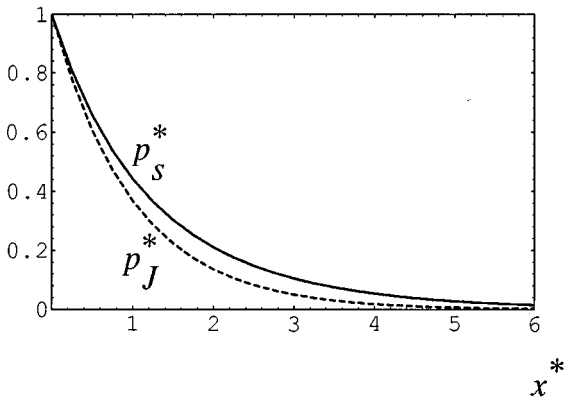

FIG. 5. Dimensionless final pressure profile when grains have stopped, $p_s^* = p_s(x)/p_0$ (solid curve), and dimensionless pressure profile of the Janssen model $p_J^* = p_J(x)/p_0$ (dashed curve), as functions of the dimensionless abscissa $x^* = x/\lambda$.

Hence the condition (19) becomes

$$\left|\frac{dp_s}{dx}\right| \leqslant \frac{p_s}{\lambda}.$$

Hypothesis (H) is correct if this equation is verified. The quantity $\lambda/p_s dp_s/dx$ is plotted in Fig. 6 as a function of x; its value always lies between -1 and $+1$. Hence hypothesis (H) is correct, i.e., grains definitively stop at $x = x_s(t)$.

Physically, the point $x_s(t)$ corresponds to a stopping front where the grain motion stops definitively, and this front propagates to the positive x direction. Grains behind this front ($x < x_s$) have already stopped, and grains ahead of it ($x > x_s$) are still moving. A grain slice located at x stops at a time t so that $x = x_s(t)$, or $t = t_s(x)$ where t_s is the inverse function of x_s. After the slice has stopped, its pressure does not change any more, and is equal to

$$p_s(x) = p[x, t_s(x)], \tag{21}$$

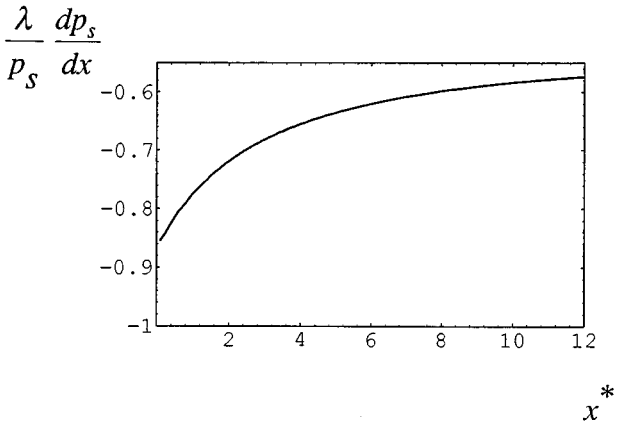

FIG. 6. $[\lambda/p_s(x)]dp_s(x)/dx$ as a function of the dimensionless abscissa $x^* = x/\lambda$. This quantity always lies between -1 and $+1$, so that static friction is sufficient to maintain the grain slices at rest after they have stopped.

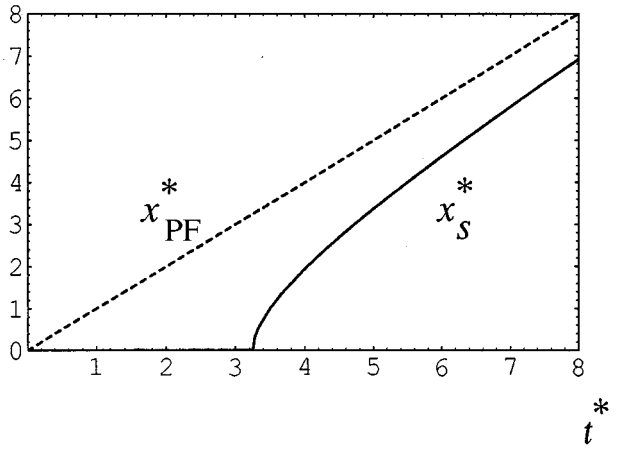

FIG. 7. Dimensionless abscissa of the pressure front $x^*_{pf} = x_{pf}(t)/\lambda = ct/\lambda$ (dashed curve) and of the stopping front $x^*_s = x_s(t)/\lambda$ (solid curve), as functions of the dimensionless time $t^* = tc/\lambda$. The grain slices at a place and a time represented by a point above the two curves have not started to move yet; the slices between the curves are moving; the slices below the curves have already stopped.

where $p(x,t)$ is the analytical solution (17). The function $p_s(x)$ can be numerically calculated using Eq. (21); this function is plotted in Fig. 5 (solid curve).

The stopping front starts from $x = 0$ at $t = t_s(x = 0) = 3.25\lambda/c$. Figure 7 shows the pressure front (where grains start to move) and the stopping front positions as functions of time. The stopping front tends to catch up with the pressure front, but always remains behind it. In Fig. 7 the area above the two curves corresponds to grains that the pressure front has not reached yet ($ct < x$); their pressure is equal to 0. Grains in the area in between the two curves $[x_s(t) < x < ct]$ are moving with a positive velocity; their pressure is given by the analytical solution (17). The stopping front has already reached the grains in the part below the two curves $[x < x_s(t)]$. These grains do not move any more, and have a pressure equal to $p_s(x)$. Figure 8 represents pressure against time at a given abscissa x, for $x = \lambda$, 2λ, and 4λ. For each curve the pressure is equal to zero until the pressure front arrives (at $t = x/c$); it then jumps to $p_0 \exp(-x/2\lambda)$, decreases during a time lag of $t_s(x) - x/c$, and stops changing when the stopping front arrives at $t = t_s(x)$. These three curves are horizontal sections of Fig. 7. Pressure against the abscissa at a given time t, for $t = \lambda/c$, $4\lambda/c$, and $5\lambda/c$, is plotted in Fig. 9. The pressure front is at the right end of the curves. These three curves are vertical sections of Fig. 7.

The final pressure of grains $p_s(x)$ is plotted in Fig. 5 (solid curve). Let us compare it with the pressure profile predicted by the Janssen model described in Sec. II of the present paper. With the boundary condition $p(x = 0) = p_0$ and when there is no gravity force, the Janssen model predicts that pressure is given by [see Eq. (3)]

$$p_J(x) = p_0 \exp\left(-\frac{x}{\lambda}\right).$$

This function is represented by a dashed curve in Fig. 5.

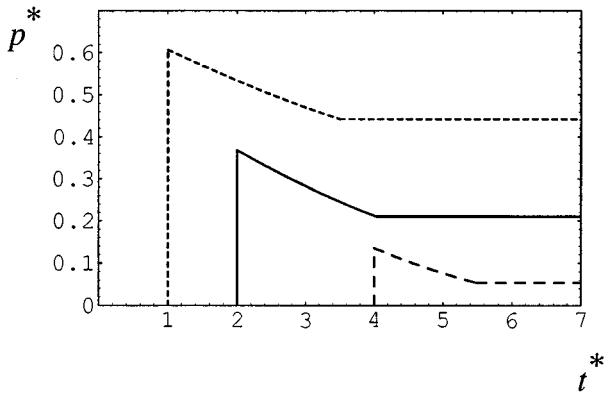

FIG. 8. Dimensionless pressure $p^*=p(x,t)/p_0$, calculated by taking into account the stopping front, as a function of the dimensionless time $t^*=tc/\lambda$, for three values of the abscissa x: $x=\lambda$ (short dashed curve), $x=2\lambda$ (solid curve), and $x=4\lambda$ (long dashed curve). The sudden increases at the left ends of the curves happen when the pressure front arrives, and the sudden stops of the decrease happen when the stopping front arrives.

Note that $p_J(x)$ decreases more quickly than does $p_s(x)$, but qualitatively the two curves are close. The best fit of $p_s(x)$ by an exponential function is

$$p_s(x)\approx p_0\exp\left(-\frac{x}{1.3\lambda}\right).$$

The characteristic damping length of $p_s(x)$, 1.3λ, is a bit larger than the damping length of $p_J(x)$, λ. This comes from the assumptions made about the static friction of grains at the cylinder sides: Eq. (20) ($dp/dx=f_{\text{stat}}$) shows that the pressure along the cylinder decreases because of this friction. Janssen assumed that this friction was maximum, whereas we did not. Hence pressure decreases more quickly in the Janssen model. Despite this small difference of the damping lengths, our final pressure distribution and the Janssen one are quite similar. This result is a bit surprising since the two models are different, our model taking into account both dynamic and static frictions. The final pressure distribution $p_s(x)$ cannot be obtained by simply setting $\partial p/\partial t=0$ in Eq. (8), since the friction term $-(1/\lambda)\partial p/\partial x$ is valid only when the grains are moving. Therefore, even if the functions $p_J(x)$ and $p_s(x)$ are close, we emphasize that these two pressure distributions are not identical.

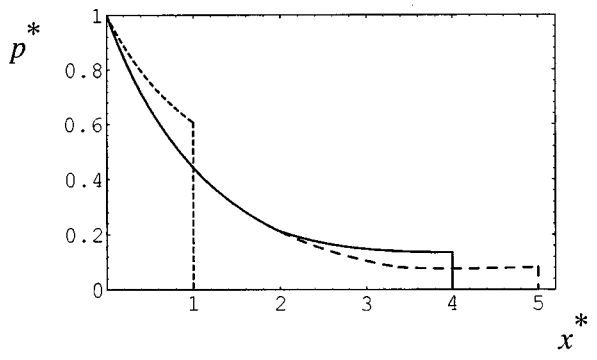

FIG. 9. Dimensionless pressure $p^*=p(x,t)/p_0$, calculated by taking into account the stopping front, as a function of the dimensionless abscissa $x^*=x/\lambda$, for three values of the time t: $t=\lambda/c$ (short dashed curve), $t=4\lambda/c$ (solid curve), and $t=5\lambda/c$ (long dashed curve). The last two curves are identical for $x^*<2.0$ since in this part of both curves, grains have already stopped: dimensionless pressure does not vary any more, and is equal to $p_s^*(x)$. Note the small break of the slope occurring at $x^*=3.4$ in the long dashed curve $t=5\lambda/c$; this break corresponds to the stopping front. A similar effect (hardly visible in the figure) occurs at $x^*=2.0$ in the solid curve $t=4\lambda/c$.

VI. CONCLUSION

In order to understand the role of wall friction on acoustic propagation in a granular medium, we have modeled the propagation of a pressure step in a cylinder filled with a granular material. In the frictionless case ($1/\lambda=0$), the pressure front would propagate at the speed of sound, and would not be damped. All grains behind the front would move at a uniform and constant speed. In the presence of solid friction between the grains and the cylinder walls, we have shown that a pressure front still propagates and that its speed is the same as in the frictionless case. Yet its amplitude is exponentially damped, and all grain slices move only during a limited time. The grain motion stops when a stopping front arrives. This front propagates behind the pressure front; its speed is always larger than the speed of sound c, but approaches c as the stopping front catches up with the pressure front. Note that the stopping front is due to friction and does not exist in the frictionless case (t_s tends to infinity as friction goes to zero). The final pressure profile of grains that we predict when they have stopped is similar but not identical to the Janssen one. In all our study, we assumed that the elastic response of the material was linear [i.e., $m=1$ in Eq. (6)]. As a consequence, the speed of sound in the material was a constant. Our conclusions should not be seriously affected if nonlinear wave propagation [29] is incorporated. We plan to study this subject in the future.

In order to neglect reflections of the pressure step on the right end of the cylinder, we assumed that the container was semi-infinite. Let us assess the minimum length that the cylinder should have in practice. We have shown that the pressure of a grain slice at position x was maximal when the pressure front arrived, and was equal to $p_0\exp(-x/2\lambda)$, where $\lambda\approx 5R$ (R being the cylinder radius). Experimentally, reflections will be negligible if they happen in an area where this maximal pressure is small compared to p_0. Hence the cylinder length should exceed ~ 30 times its radius.

Let us end this paper by considering, from a practical point of view, the filling of a vertical silo (we take into account the grain weight). We assume that the granular material is poured with a constant ingoing flux Q. This situation is similar to the one represented in Fig. 1, with a grain height increasing at a constant speed $V=Q/\pi R^2$. Let us now take $x=0$ at the container's bottom, so that grains are located at $-Vt\leqslant x\leqslant 0$. Let us try to determine $p(x,t)$ and $v(x,t)$ during the filling. The differential equations are

$$\rho c^2\frac{\partial v}{\partial x}=-\frac{\partial p}{\partial t}$$

and

$$\rho \frac{\partial v}{\partial t} = -\frac{\partial p}{\partial x} - \frac{p}{\lambda} + \rho g. \tag{22}$$

The only difference with Eqs. (7) and (5) for the pressure step propagation in a horizontal cylinder is the gravity term ρg added in Eq. (22). The friction term $-p/\lambda$ in Eq. (22) is again negative since the poured grains are progressively compressed and we expect a positive velocity. The boundary conditions are now $v(x=0,t)=0$, and $p(x=-Vt,t)=0$: grains that are being poured in the silo at the top of the granular material have a negligible pressure. Determining the exact analytical solution of this model is a difficult mathematical problem. We do not expect any more that a stopping front propagates when the cylinder is filled with a constant flux. We propose two different approximations for two different regimes: a short time regime when the filling starts ($t<\lambda/V$), and a long time regime ($t>\lambda/V$). In both regimes, the expressions of p and v will be simplified, assuming that $V \ll c$.

(i) In the short time regime ($t<\lambda/V$), the grain height in the cylinder is smaller than the characteristic damping length λ of friction, and we can neglect the friction term $-p/\lambda$ in Eq. (22). It is then easy to obtain

$$p\left(x,t<\frac{\lambda}{V}\right) = \rho g(x+Vt),$$

$$v\left(x,t<\frac{\lambda}{V}\right) = \frac{gV}{c^2}(-x).$$

The pressure is the same as in a liquid at rest. The speed does not depend on time t, provided that $t<\lambda/V$. Note that as expected, we have $v>0$ since x is negative.

(ii) In the long time regime ($t>\lambda/V$) and in the frame moving up at the velocity V with respect to the silo frame, we expect that both p and v hardly depend on time, especially in the upper part of the granular material. So in the silo frame we can try to find a solution of the following kind: $p(x,t)=p(x+Vt)$, and $v(x,t)=v(x+Vt)$. Using the two partial differential equations and the boundary conditions, we get

$$p\left(x,t>\frac{\lambda}{V}\right) = \rho g\lambda\left[1-\exp\left(-\frac{x+Vt}{\lambda}\right)\right],$$

$$v\left(x,t>\frac{\lambda}{V}\right) = \frac{gV}{c^2}\lambda\exp\left(-\frac{x+Vt}{\lambda}\right).$$

The pressure p is a Janssen pressure distribution, shifted up at the constant velocity V as the upper grain surface ($x=-Vt$). Note that this expression for the velocity does not exactly satisfy the boundary condition $v(x=0,t)=0$, but tends to satisfy it in the very long time limit.

What happens when we stop the ingoing flux Q at a time t_0 after having poured a given height of grains? Work is still in progress in order to determine $p(x,t>t_0)$ and $v(x,t>t_0)$. We expect that as the speed progressively tends to zero, the grain compression goes on and the pressure in the granular medium increases.

ACKNOWLEDGMENTS

We acknowledge very interesting discussions with J. Duran. We also want to thank C. Gay and M. Hébert for very useful comments.

APPENDIX A: GREEN'S FUNCTION

We shall determine the Green function of the linear differential operator

$$L = \frac{1}{c^2}\frac{\partial^2}{\partial t^2} - \frac{\partial^2}{\partial x^2} - \frac{1}{\lambda}\frac{\partial}{\partial x},$$

using standard methods of mathematical physics [24,25]. The Green function $G(x,t)$ must satisfy the equation

$$LG = \delta(x)\,\delta(t), \tag{A1}$$

where δ is the Dirac delta function. Let us define a new function $F(x,t)$ as

$$F(x,t) = \exp\left(\frac{x}{2\lambda}\right) G(x,t).$$

For $F(x,t)$, the differential equation (A1) becomes

$$\left(\frac{1}{c^2}\frac{\partial^2}{\partial t^2} - \frac{\partial^2}{\partial x^2} + \frac{1}{4\lambda^2}\right) F(x,t) = \delta(x)\,\delta(t).$$

The Fourier transform $\hat{F}(k,t)=\int_{-\infty}^{+\infty} dx \exp(-ikx) F(x,t)$ satisfies

$$\frac{1}{c^2}\frac{\partial^2 \hat{F}}{\partial t^2} + \left(k^2 + \frac{1}{4\lambda^2}\right)\hat{F} = \delta(t). \tag{A2}$$

The most general solution of the corresponding homogeneous equation

$$\frac{1}{c^2}\frac{\partial^2 \hat{F}_0}{\partial t^2} + \left(k^2 + \frac{1}{4\lambda^2}\right)\hat{F}_0 = 0$$

is equal to

$$\hat{F}_0(k,t) = a_1(k)\sin\left(\sqrt{k^2+\frac{1}{4\lambda^2}}\,ct\right) + a_2(k)\cos\left(\sqrt{k^2+\frac{1}{4\lambda^2}}\,ct\right),$$

where $a_1(k)$ and $a_2(k)$ are arbitrary functions. A particular solution of Eq. (A2) is given by

$$\hat{F}_{\text{part}} = \theta(t)\hat{F}_0,$$

where θ is the Heaviside unit step function. We find that $\hat{F}_{\text{part}}$ is a solution of Eq. (A2) when a_1 and a_2 are given by

$$a_1(k)=\frac{c}{\sqrt{k^2+1/4\lambda^2}} \quad \text{and} \quad a_2(k)=0.$$

The solution of Eq. (A2) which fulfills the causality condition is then given by

$$\hat{F}(k,t)=\frac{c}{\sqrt{k^2+1/4\lambda^2}}\,\theta(t)\sin\left(\sqrt{k^2+\frac{1}{4\lambda^2}}ct\right).$$

Returning to real space, we obtain

$$F(x,t)=\frac{c}{2}\,\theta(ct-|x|)J_0\left(\frac{\sqrt{c^2t^2-x^2}}{2\lambda}\right),$$

where J_0 is a Bessel function of the first kind [26]. Indeed it is easy to verify that

$$\int_{-\infty}^{+\infty}dx\exp(-ikx)\frac{c}{2}\,\theta(ct-|x|)J_0\left(\frac{\sqrt{c^2t^2-x^2}}{2\lambda}\right)=\frac{c}{2}\,\theta(t)\int_{-ct}^{+ct}dx\exp(-ikx)J_0\left(\frac{\sqrt{c^2t^2-x^2}}{2\lambda}\right)$$

$$=c\,\theta(t)\int_0^{ct}dx\cos(kx)J_0\left(\frac{\sqrt{c^2t^2-x^2}}{2\lambda}\right)=c\,\theta(t)\,\frac{\sin(\sqrt{k^2+1/4\lambda^2}ct)}{\sqrt{k^2+1/4\lambda^2}}.$$

See Ref. [30] for the last step. In conclusion, for the linear differential operator L, the Green function is given by

$$G(x,t)=\frac{c}{2}\,\theta(ct-|x|)\exp\left(-\frac{x}{2\lambda}\right)J_0\left(\frac{\sqrt{c^2t^2-x^2}}{2\lambda}\right).$$

APPENDIX B: SOLUTION OF THE CAUCHY PROBLEM

Let us consider the differential equation

$$\frac{1}{c^2}\frac{\partial^2 p_C}{\partial t^2}-\frac{\partial^2 p_C}{\partial x^2}-\frac{1}{\lambda}\frac{\partial p_C}{\partial x}=0.$$

We assume we know $p_C(x,t=0)$ and $(\partial p_C/\partial t)(x,t=0)$, and we want to determine $p_C(x,t\geqslant 0)$ (i.e., we want to solve the Cauchy problem for this differential equation). We have shown that the solution is equal to the convolution product

$$p_C(x,t\geqslant 0)=A(x,t)*G(x,t),$$

where

$$A(x,t)=\frac{1}{c^2}\left[\delta(t)\frac{\partial p_C}{\partial t}(x,t=0)+\delta'(t)p_C(x,t=0)\right],$$

$$G(x,t)=\frac{c}{2}\,\theta(ct-|x|)\exp\left(-\frac{x}{2\lambda}\right)J_0\left(\frac{\sqrt{c^2t^2-x^2}}{2\lambda}\right).$$

We shall calculate this convolution product. In order to shorten the mathematical expressions, we shall define $u_0(x)$ and $u_1(x)$ by

$$u_0(x)=\frac{1}{c^2}p_C(x,t=0) \quad \text{and} \quad u_1(x)=\frac{1}{c^2}\frac{\partial p_C}{\partial t}(x,t=0).$$

Let us calculate the first part P_1 of the convolution product

$$P_1=[\delta(t)u_1(x)]*G(x,t)=\int_{-\infty}^{+\infty}dx'\int_{-\infty}^{+\infty}dt'\,\delta(t')u_1(x')G(x-x',t-t')$$

$$=\frac{c}{2}\int_{-\infty}^{+\infty}dx'u_1(x')\;\theta(ct-|x-x'|)\exp\left(-\frac{x-x'}{2\lambda}\right)J_0\left(\frac{\sqrt{c^2t^2-(x-x')^2}}{2\lambda}\right)$$

$$=\frac{c}{2}\,\theta(t)\int_{x-ct}^{x+ct}dx'u_1(x')\exp\left(\frac{x'-x}{2\lambda}\right)J_0\left(\frac{\sqrt{c^2t^2-(x'-x)^2}}{2\lambda}\right).$$

The second part P_2 of the convolution product is equal to

$$P_2=[\delta'(t)u_0(x)]*G(x,t)=\int_{-\infty}^{+\infty}dx'\int_{-\infty}^{+\infty}dt'\,\delta'(t-t')u_0(x-x')G(x',t')=\frac{\partial}{\partial t}\{[\delta(t)u_0(x)]*G(x,t)\}.$$

By using the expression of P_1, we obtain

$$\begin{aligned}P_2&=\frac{\partial}{\partial t}\left\{\frac{c}{2}\,\theta(t)\int_{x-ct}^{x+ct}dx'u_0(x')\exp\left(\frac{x'-x}{2\lambda}\right)J_0\left(\frac{\sqrt{c^2t^2-(x'-x)^2}}{2\lambda}\right)\right\}\\&=-\frac{c}{2}\,\theta(t)\int_{x-ct}^{x+ct}dx'u_0(x')\exp\left(\frac{x'-x}{2\lambda}\right)\frac{c^2t}{2\lambda}\,\frac{J_1((1/2\lambda)\sqrt{c^2t^2-(x'-x)^2})}{\sqrt{c^2t^2-(x'-x)^2}}\\&\quad+\frac{c^2}{2}\,\theta(t)\left[u_0(x+ct)\exp\left(\frac{ct}{2\lambda}\right)+u_0(x-ct)\exp\left(-\frac{ct}{2\lambda}\right)\right].\end{aligned}$$

To derive the last expression, we used the formula

$$J_0(0)=1\quad\text{and}\quad J_0'(x)=-J_1(x),$$

where $J_1(x)$ is a Bessel function of the first kind [26]. The solution of the Cauchy problem is finally given by

$$\begin{aligned}p_C(x,t\geqslant 0)&=\frac{1}{2c}\int_{x-ct}^{x+ct}dx'\,\frac{\partial p_C}{\partial t}(x',0)\exp\left(\frac{x'-x}{2\lambda}\right)J_0\left(\frac{\sqrt{c^2t^2-(x'-x)^2}}{2\lambda}\right)-\frac{ct}{4\lambda}\int_{x-ct}^{x+ct}dx'p_C(x',0)\\&\quad\times\exp\left(\frac{x'-x}{2\lambda}\right)\frac{J_1((1/2\lambda)\sqrt{c^2t^2-(x'-x)^2})}{\sqrt{c^2t^2-(x'-x)^2}}+\frac{1}{2}\left[p_C(x+ct,0)\exp\left(\frac{ct}{2\lambda}\right)+p_C(x-ct,0)\exp\left(-\frac{ct}{2\lambda}\right)\right].\end{aligned}$$

APPENDIX C: A SIMPLE EXPRESSION FOR THE PRESSURE

In our water hammer model for a granular material, the grain pressure is given by

$$\begin{aligned}p(x,t\geqslant 0)&=p_0+\frac{1}{2}\left[p_C(x+ct,0)\exp\left(\frac{ct}{2\lambda}\right)+p_C(x-ct,0)\exp\left(-\frac{ct}{2\lambda}\right)\right]\\&\quad-\frac{ct}{4\lambda}\int_{x-ct}^{x+ct}dx'p_C(x',0)\exp\left(\frac{x'-x}{2\lambda}\right)\frac{J_1((1/2\lambda)\sqrt{c^2t^2-(x'-x)^2})}{\sqrt{c^2t^2-(x'-x)^2}},\end{aligned}$$

where

$$p_C(x,0)=\begin{cases}p_0\exp\left(-\dfrac{x}{\lambda}\right) & \text{if } x<0\\[2ex] -p_0 & \text{if } x>0.\end{cases}$$

We shall simplify this expression for $t\geqslant x/c$,

$$\begin{aligned}p\left(x,t\geqslant\frac{x}{c}\right)&=p_0+\frac{p_0}{2}\left[-\exp\left(\frac{ct}{2\lambda}\right)+\exp\left(\frac{ct-x}{\lambda}\right)\exp\left(-\frac{ct}{2\lambda}\right)\right]-\frac{ct}{4\lambda}\int_{-ct}^{+ct}dx'p_C(x'+x,0)\exp\left(\frac{x'}{2\lambda}\right)\frac{J_1((1/2\lambda)\sqrt{c^2t^2-x'^2})}{\sqrt{c^2t^2-x'^2}}\\&=p_0\left\{1+\frac{1}{2}\exp\left(\frac{ct}{2\lambda}\right)\left[\exp\left(-\frac{x}{\lambda}\right)-1\right]\right\}-p_0\frac{ct}{4\lambda}\left[\int_{-ct}^{-x}dx'\exp\left(-\frac{x'+x}{\lambda}\right)\exp\left(\frac{x'}{2\lambda}\right)\frac{J_1((1/2\lambda)\sqrt{c^2t^2-x'^2})}{\sqrt{c^2t^2-x'^2}}\right.\\&\quad\left.-\int_{-x}^{ct}dx'\exp\left(\frac{x'}{2\lambda}\right)\frac{J_1((1/2\lambda)\sqrt{c^2t^2-x'^2})}{\sqrt{c^2t^2-x'^2}}\right].\end{aligned}\tag{C1}$$

In order to shorten the mathematical expressions, we define the following dimensionless quantities:

$$\tau=\frac{ct}{2\lambda},\quad\chi=\frac{x}{2\lambda},\quad\text{and}\quad\chi'=\frac{x'}{2\lambda}.$$

Then the equality (C1) can be rewritten

$$\frac{p(\chi,\tau\geqslant\chi)}{p_0}=1+\frac{\exp(\tau)}{2}[\exp(-2\chi)-1]-\frac{\tau}{2}\left[\int_{-\tau}^{-\chi}d\chi'\exp(-2\chi-\chi')\frac{J_1(\sqrt{\tau^2-\chi'^2})}{\sqrt{\tau^2-\chi'^2}}-\int_{-\chi}^{-\tau}d\chi'\exp(\chi')\frac{J_1(\sqrt{\tau^2-\chi'^2})}{\sqrt{\tau^2-\chi'^2}}\right.$$
$$\left.-\int_{-\tau}^{+\tau}d\chi'\exp(\chi')\frac{J_1(\sqrt{\tau^2-\chi'^2})}{\sqrt{\tau^2-\chi'^2}}\right]$$
$$=1+\frac{\exp(\tau)}{2}[\exp(-2\chi)-1]-\frac{\tau}{2}\int_{-\tau}^{-\chi}d\chi'\exp(-\chi)[\exp(\chi+\chi')+\exp(-\chi-\chi')]\frac{J_1(\sqrt{\tau^2-\chi'^2})}{\sqrt{\tau^2-\chi'^2}}$$
$$+\frac{\tau}{2}\int_{-\tau}^{+\tau}d\chi'\exp(\chi')\frac{J_1(\sqrt{\tau^2-\chi'^2})}{\sqrt{\tau^2-\chi'^2}}.$$

The last expression of p/p_0 is a sum of three terms. Let us call them successively T_1, T_2, and T_3. Let us first simplify the term T_2,

$$T_2=-\tau\int_{-\tau}^{-\chi}d\chi'\exp(-\chi)\cosh(\chi+\chi')\frac{J_1(\sqrt{\tau^2-\chi'^2})}{\sqrt{\tau^2-\chi'^2}}$$
$$=-\tau\exp(-\chi)\int_{\chi/\tau}^{1}dz\cosh(z\tau-\chi)\frac{J_1(\tau\sqrt{1-z^2})}{\sqrt{1-z^2}}.$$

Then the term T_3 is equal to

$$T_3=\frac{\tau}{2}\int_{-\tau}^{+\tau}d\chi'\exp(\chi')\frac{J_1(\sqrt{\tau^2-\chi'^2})}{\sqrt{\tau^2-\chi'^2}}$$
$$=\tau\int_{0}^{\tau}d\chi'\cosh(\chi')\frac{J_1(\sqrt{\tau^2-\chi'^2})}{\sqrt{\tau^2-\chi'^2}}$$
$$=\cosh(\tau)-1.$$

See Ref. [30] for the last derivation. The sum of the terms T_1 and T_3 is

$$T_1+T_3=1+\frac{\exp(\tau)}{2}[\exp(-2\chi)-1]+\cosh(\tau)-1$$
$$=\exp(-\chi)\cosh(\tau-\chi).$$

Hence $p(\chi,\tau\geqslant\chi)$ is given by

$$p(\chi,\tau\geqslant\chi)=p_0\exp(-\chi)\left[\cosh(\tau-\chi)-\tau\int_{\chi/\tau}^{1}dz\cosh(z\tau-\chi)\frac{J_1(\tau\sqrt{1-z^2})}{\sqrt{1-z^2}}\right].$$

Using the quantities with dimensions, $p(x,t\geqslant x/c)$ is finally given by

$$p\left(x,t\geqslant\frac{x}{c}\right)=p_0\exp\left(-\frac{x}{2\lambda}\right)\left[\cosh\left(\frac{ct-x}{2\lambda}\right)-\frac{ct}{2\lambda}\times\int_{x/ct}^{1}dz\cosh\left(\frac{zct-x}{2\lambda}\right)\frac{J_1((ct/2\lambda)\sqrt{1-z^2})}{\sqrt{1-z^2}}\right].$$

[1] J.M. Marchello, *Gas-Solid Handling in the Process Industries* (Marcel Dekker, New York, 1976).
[2] R.A. Bagnold, *The Physics of Blown Sand and Desert Dunes* (Methuen, London, 1941).
[3] H.M. Jaeger and S.R. Nagel, Science **255**, 1523 (1992).
[4] C.H. Lui *et al.*, Science **269**, 513 (1995).
[5] A. Mehta, *Granular Matter* (Springer-Verlag, Berlin, 1994); J.P. Bouchaud, M.E. Cates, J. Ravi Prakash, and S.F. Edwards, J. Phys. (France) I **4**, 1383 (1994); T. Boutreux and P.G. de Gennes, *ibid.* **6**, 1295 (1996).
[6] J. Duran, J. Rajchenbach, and E. Clément, Phys. Rev. Lett. **70**, 2431 (1993).
[7] D.E. Wolf, in *Computational Physics*, edited by K.H. Hoffmann and M. Schreiber (Springer, Heidelberg, 1996).
[8] H.A. Janssen, Z. Ver. Dsch. Ing. **39**, 1045 (1895).
[9] G.K. Batchelor, *An Introduction to Fluid Dynamics* (Cambridge University Press, Cambridge, England, 1967).
[10] T. Wakabayashi, *Proceedings of the Ninth Japanese National Congress on Applied Mechanics* (Science Council of Japan, Tokyo, 1960).
[11] M. Ammi, T. Travers, and J.P. Troades, J. Phys. D **20**, 424 (1987).
[12] C.E.D. Ouwerkerk, Powder Technol. **65**, 125 (1991).
[13] R.L. Brown and J.C. Richards, *Principles of Powder Mechanics* (Pergamon, New York, 1966).
[14] R.A. Saul, Agric. Eng. **34**, 231 (1953).
[15] D. Lenczner, Mag. Concr. Res. **15**, 101 (1963).
[16] S.F. Edwards and R.B.S. Oakeshott, Physica D **38**, 88 (1989).
[17] P.G. de Gennes (unpublished).
[18] J.D. Goddard, Proc. R. Soc. London, Ser. A **430**, 105 (1990).
[19] J. Duffy and R.D. Mindlin, J. Appl. Mech. **24**, 585 (1957).
[20] P.G. de Gennes, *Lectures on Granular Matter at the Varenna*

School (July 1996), (Societa Italiana di Fisica, Bologna, in press).
[21] C-h. Liu and S.R. Nagel, Phys. Rev. Lett. **68**, 2301 (1992).
[22] J. Duran, *Sables, Poudres et Grains* (Eyrolles, Paris, 1997) (in French).
[23] J. Duran (private communication).
[24] P.M. Morse and H. Feshbach, *Methods of Theoretical Physics* (McGraw-Hill, New York, 1953).
[25] V.S. Vladimirov, *Equations of Mathematical Physics* (Marcel Dekker, New York, 1971).
[26] *Handbook of Mathematical Functions*, edited by M. Abramowitz and I.A. Stegun (Dover Publications, New York, 1965).
[27] A.R. Mitchell and D.F. Griffiths, *The Finite Difference Method in Partial Differential Equations* (Wiley, New York, 1980).
[28] D. Euvrard, *Résolution Numérique des Equations aux Dérivées Partielles*, 3rd ed. (Masson, Paris, 1994) (in French).
[29] The effect of a nonlinear elasticity on sound propagation has recently been studied by Sinkovits and Sen [R.S. Sinkovits and S. Sen, Phys. Rev. Lett. **74**, 2686 (1995)]. The effect of wall friction was not considered by these authors, however.
[30] I.S. Gradshteyn and I.M. Ryzhik, *Table of Integrals, Series, and Products* (Academic Press, New York, 1980). See the chapter on definite integrals of Bessel functions.